membrane. Presumably, this is accomplished via a local conformational change in the B-subunits. This paper has addressed the changes in the toxin molecule induced by the oligosaccharide portion of ganglioside G_{M1}. The other aspect of this association is the effect on the lipidic portion of the ganglioside, its propagation to the lipid bilayer, as well as the effects resulting from the formation of a protein–membrane interface. These topics are currently under investigation in this laboratory. Preliminary calorimetric experiments performed with intact ganglioside G_{M1} incorporated into phospholipid vesicles are consistent with an overall enthalpy of binding on the order of −85 kcal/mol of toxin (A. Schön, unpublished results). These results suggest that the binding of the B-subunit to the oligosaccharide region of ganglioside G_{M1} affects both the intersubunit protein interactions and the lipid interactions. The additional endothermic effect of ~70 kcal/mol observed with membrane-bound intact ganglioside is consistent with the conclusion of Ribi et al. (1988) of a reduced lipid packing density beneath the B-subunit pentamer. Whether these additional effects are transduced through the lipidic portion of ganglioside G_{M1} or arise as a direct result of the attachment of the protein to the membrane surface is still unknown.

Registry No. Ganglioside G_{M1}, 37758-47-7.

References

Dalziel, A. W., Lipka, G., Chowdhry, B. Z., Sturtevant, J. M., & Schafer, D. E. (1984) *Mol. Cell. Biochem. 63*, 83–91.

Dani, M., Manca, F., & Rialdi, G. (1981) *Biochim. Biophys. Acta 667*, 108–117.

De Wolf, M. J. S., Fridkin, M., Epstein, M., & Kohn, L. D. (1981) *J. Biol. Chem. 256*, 5481–5488.

Fishman, P. H., Moss, J., & Osborne, J. C., Jr. (1978) *Biochemistry 17*, 711–716.

Gill, D. M. (1976) *Biochemistry 15*, 1242–1248.

Goins, B., & Freire, E. (1985) *Biochemistry 24*, 1791–1797.

Goins, B., Masserini, M., Barisas, B. G., & Freire, E. (1986) *Biophys. J. 49*, 849–856.

Goins, B., & Freire, E. (1988) *Biochemistry 27*, 2046–2052.

Goins, B., & Freire, E. (1988) in *New Trends in Ganglioside Research* (Ledeen, R. W., Hogan, E. L., Tettamanti, G., & Yates, A. J., Eds.) Fidia Research Series, Vol. 14, Liviana Press, Padova, Italy.

Ito, M., & Yamagata, T. (1986) *J. Biol. Chem. 261*, 14278–14282.

Lowry, O. H., Rosebrough, N. J., Farr, A. L., & Randall, R. J. (1951) *J. Biol. Chem. 193*, 265–275.

Masserini, M., & Freire, E. (1987) *Biochemistry 26*, 237–242.

Myers, M., Mayorga, O. L., Emtage, J., & Freire, E. (1987) *Biochemistry 26*, 4309–4315.

Ribi, H. D., Ludwig, D. S., Mercer, K. L., Schoolnik, G. K., & Kornberg, R. D. (1988) *Science 239*, 1272–1276.

Sattler, J., Schwartzmann, G., Knack, I., Röhm, K.-H., & Wiegandt, H. (1978) *Hoppe-Seyler's Z. Physiol. Chem. 359*, 719–723.

Schafer, D. E., & Thakur, A. K. (1982) *Cell Biophys. 4*, 25–40.

Spiro, R. G. (1966) *Methods Enzymol. 8*, 1–52.

Staerck, J., Ronneberger, H. J., Wiegandt, H., & Ziegler, W. (1974) *Eur. J. Biochem. 48*, 103–110.

Wisnieski, B. J., & Bramhall, J. S. (1981) *Nature (London) 289*, 319–321.

Carbon-13 NMR of Glycogen: Hydration Response Studied by Using Solids Methods†

Cynthia L. Jackson and Robert G. Bryant*

Department of Chemistry and Department of Biophysics, University of Rochester, Rochester, New York 14642

Received February 1, 1989

ABSTRACT: The carbon-13 NMR spectra of glycogen are reported by using the methods of magic-angle sample spinning and high-power proton decoupling to provide a dynamic report on the glucose monomer behavior as a function of hydration. Although the glycogen behaves as a typical polymer in the dry state, addition of water makes a significant difference in the spectral appearance. Water addition decreases the carbon spin–lattice relaxation times by 2 orders of magnitude over the range from 7% to 70% water by weight. The proton–carbon dipole–dipole coupling, which broadens the carbon spectrum and permits cross-polarization spectroscopy, is lost with increasing hydration over this range. By 60% water by weight, scalar decoupling methods are sufficient to achieve a reasonably high-resolution spectrum. Further, at this concentration, the carbon spin–lattice relaxation times are near their minimum values at a resonance frequency of 50.3 MHz, making acquisition of carbon spectra relatively insensitive to intensity distortions associated with saturation effects. Though motional averaging places the spectrum in the solution phase limit, the static spectrum shows a residual broader component that would not necessarily be detected readily by using high-resolution liquid-state experiments.

Glycogen is a branched glucose polymer of variable molecular weight that typically ranges from 400 000 to 700 000 in vivo. The glycogen backbone is an α-1,4-glycosidic structure with branch points α-1,6 approximately every 8–12 glucose residues (Metzler, 1977). Since glycogen is a glucose storage molecule, it is important for metabolic studies of carbohydrate metabolism (Cohen et al., 1981; Stevens et al., 1982; Canioni et al., 1983; Sillerud & Shulman, 1983; Neurohr et al., 1984; Reo et al., 1984). As a branched polysaccharide, this molecule represents an important class of molecules that are significantly different from more collapsed structure macromolecules such

† This work was supported by the National Institutes of Health (GM-14534 and CA-40699) and the University of Rochester.

* Address correspondence to this author at the Department of Biophysics, University of Rochester Medical Center, Rochester, NY 14642.

0006-2960/89/0428-5024$01.50/0 © 1989 American Chemical Society

as proteins. The dynamic and structural response of glycogen to water is important for a more complete understanding of water–macromolecule interactions in general. In addition, a dynamic understanding of glycogen is crucial for interpretation of high-resolution in vivo metabolic NMR studies using labeled glucose feeds. In spite of the high molecular weights of the in vivo glucose molecules, metabolic studies using C-1-labeled glucose report little or no apparent signal loss from C-1-labeled glucose when it is incorporated into glycogen and detected by using high-resolution methods (Cohen et al., 1981). These observations raise a fundamental question concerning the basis for the glycogen observability in such experiments. Solid-state NMR techniques permit observation of all carbon resonances regardless of their dynamic state, and thus provide a direct means for addressing this question as well as characterizing the glycogen molecular dynamics. Since there is no doubt that solid glycogen is unobservable in the usual high-resolution spectrometer, the basic issue about glycogen observability and interpretation rests on the dynamic response of the polymer to perturbation by solvent, water. Similar NMR methods have been used to study the related α-1,4 starch molecules and β-1,4 cellulose molecules (Fyfe et al., 1984; Horii et al., 1986; Veregin et al., 1986; Earl & VanderHart, 1981; VanderHart & Atalla, 1984; Cael et al., 1985). We report here studies on glycogen that demonstrate the primary dynamic response to solvent addition is a dramatic increase in local segmental mobility that leads to an essentially complete loss of the proton–carbon dipole–dipole coupling when the water content exceeds 60% and this loss is accompanied by a large reduction in the carbon spin–lattice relaxation time as well.

Experimental Procedures

Carbon-13 NMR spectra were obtained on a spectrometer constructed in this laboratory, largely from commercial components, that operates at 4.7 T using an Oxford 200/98 magnet, PTS frequency synthesizers, Amplifier Research AR-200 broad-band and Henry Radio tuned rf power amplifiers, a GE-Nicolet 1280 data system, and a receiver constructed in this laboratory that uses a Miteq preamplifier, an Avantek amplifier cascade to drive a Merrimac mixer to recover the 10-MHz intermediate frequency, and a second Avantek amplifier cascade to drive a Merrimac quadrature phase comparator. A Rockland Model 452 dual-channel audio filter and amplifier precedes digitization by the Nicolet-GE 1280. The probe was constructed by using a coaxial line connecting the inductor to the proton tuning elements at a half-wavelength; the carbon rf was injected and detected at the point along the coaxial line where the proton voltage is minimum. Additional proton–carbon isolation was provided by proton traps before the carbon preamplifier and K & L high-power band-pass filters on the proton transmitter side. The preamplifier was protected in the usual way with series-crossed diodes on the transmitter side of the probe and crossed diodes to ground at a quarter wavelength from the transmitter junction. The magic-angle sample spinning was done by using a stator and rotor assembly purchased from Doty Scientific, Columbia, SC, and sealed with double O-ring rotor caps. Absence of water loss from the sample was monitored by weighing the rotor before and after the NMR experiment.

Water contents of the glycogen samples were determined gravimetrically by drying to constant weight using a mechanical vacuum pump at room temperature in addition to P_2O_5. The molecular weight of the glycogen (Sigma Chemical Co., G8751) was determined by gel filtration using a 2.75 mm × 25 mm Bio-Gel A-1.5 agarose column. The eluate collected in 2-mL fractions was assayed for carbohydrate by the phenol–sulfuric method (Dubois et al., 1956) using a Hewlett-Packard Model 8451A diode array spectrophotometer to measure the absorbance at 490 nm. Fractions were assayed for protein content by using the absorbance at 280 nm.

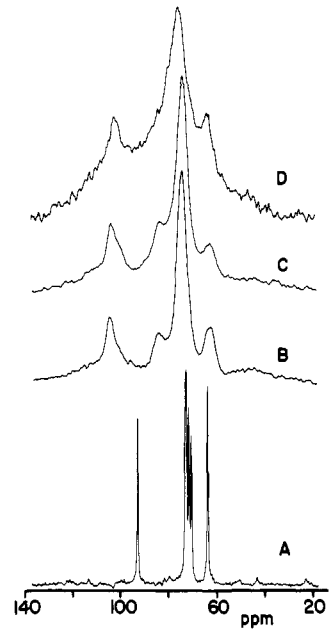

FIGURE 1: Cross-polarization magic-angle spinning carbon-13 NMR spectra obtained at 50.3 MHz referenced to TMS. (A) Anhydrous α-D-glucose using a contact time of 1 ms, 1080 transients, and 10-Hz line broadening. (B) Glycogen hydrated to 7.3% water by weight using a contact time of 750 μs, 468 transients, and a line broadening of 30 Hz. The spinning speed was 2.95 kHz. (C) Glycogen hydrated to 23.5% water by weight using a contact time of 750 μs, 360 transients, and a line broadening of 30 Hz. The spinning speed was 1.8 kHz. (D) Glycogen hydrated to 41.3% water by weight using a contact time of 750 μs, 18 296 transients, and a line broadening of 30 Hz. The spinning speed was 1.5 kHz.

Results and Discussion

The carbon-13 NMR spectrum of solid glycogen containing 7.3% water is shown in Figure 1B obtained on 43 mg of sample using magic-angle spinning and cross-polarization methods. The spectrum of solid α-D-glucose is shown in Figure 1A for comparison. Several features are immediately apparent. The crystalline glucose spectrum is similar to that of the solution, a situation characteristic of low molecular weight crystalline solids. The carbon resonances have been assigned (Pfeffer et al., 1984). The glycogen spectrum is, by comparison, poorly resolved with line widths in the several ppm range. This situation is characteristic of glassy polymers (Schaefer & Stejskal, 1979) and highly branched polymer systems in particular (English, 1985). The breadth of the polymer carbon lines is usually attributed to a considerable distribution of isotropic carbon chemical shifts that is in turn associated with a distribution of local intermolecular interactions. As in other polymers, the cross-polymerization experiment is efficient for the dry glycogen, permitting rapid acquisition of excellent spectra.

The carbon-13 NMR spectra of a series of glycogen samples are shown in Figure 1B–D and Figure 2A–C that show the effects of increasing hydration. The shape and width of the carbon resonances do not change significantly over the water content range from 7% to 30% water by weight. However, the ability to achieve an efficient cross-polarization signal at a contact time of 750 μs is compromised with increasing water content. The situation becomes increasingly severe at water contents above 30% so that the 41.3% sample provides very poor signal-to-noise ratio using cross-polarization methods.

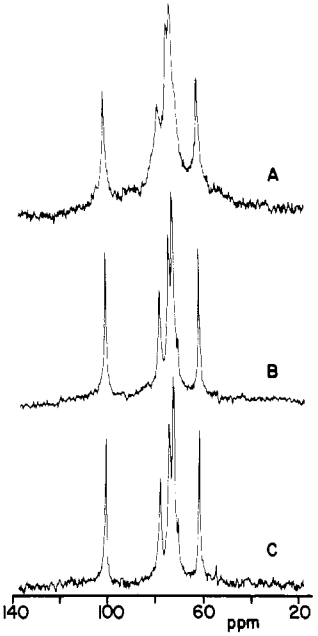

FIGURE 2: Carbon-13 NMR spectra obtained at 50.3 MHz on hydrated glycogen samples. (A) 49% water by weight obtained using magic-angle sample spinning and a 90° carbon pulse, 2676 transients, dipolar decoupling, and a line-broadening parameter of 10 Hz. The rotor frequency was 2.0 kHz. (B) 59.8% water by weight obtained using magic-angle spinning and a 90° carbon pulse, 21 584 transients, and scalar decoupling with a line-broadening parameter of 10 Hz. The rotor frequency was 1.47 kHz. (C) 72.7% water by weight using magic-angle spinning and 90° carbon pulses, 33 056 transients, scalar decoupling, and a line-broadening parameter of 10 Hz. The rotor frequency was 1.5 kHz.

Table I: Summary of Acquisition Information and Signal-to-Noise Ratio[a]

hydration (wt %)	R	sample mass (mg)	transients	mode	factor
7.3	0.76	43.4	468	CP	1
23.8	2.97	244.9	360	CP	4.94
41.8	6.81	175.5	18296	CP	25.29
49.7	9.65	160.3	2676	90°	2.21
59.8	14.4	150.2	21584	90°	5.87
72.7	25.7	152.0	33056	90°	7.36

[a] A factor of 4 is included for the change between CP and 90° pulse modes. R = ratio of moles of water to moles of glucose present in the polymer.

This loss in signal is summarized in Table I, where scaling factors are listed on the basis of the square root of the number of transients accumulated and the mass of sample in the rotor. The optimal gain in signal is also assumed in comparison of cross-polarization with carbon 90° pulse spectra, i.e., a factor of 4. The loss of signal may arise from two sources: the introduction of mobile protons into the sample could significantly alter the proton or carbon spin–lattice relaxation time in the rotating frame, T_{1rho}, a significant decrease in which would reduce the signal achieved by cross-polarization (Schaefer et al., 1980). Alternatively, the strength of the proton–carbon dipole–dipole coupling may be dramatically reduced by rapid local motions resulting in an increase in the cross-relaxation time, T_{IS} (Demco et al., 1975). That is, the buildup of carbon magnetization by contact with the proton magnetization bath will take longer. Both effects have been observed experimentally. The recovery of the spectrum for the more hydrated cases is demonstrated in spectra A, B, and C of Figure 2 which were obtained by using simple carbon 90° pulses, i.e., without magnetization transfer from the proton

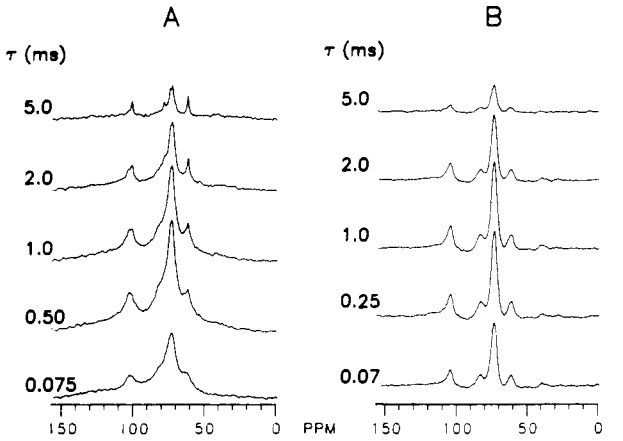

FIGURE 3: Carbon-13 CP-MASS spectra of hydrated glycogen samples obtained at 50.3 MHz as a function of contact time using 40-Hz line broadening and a rotor speed of 1.5 kHz. (A) 37.96% water by weight obtained with 10 000 transients on a sample containing 125.8 mg of glycogen. (B) 6.2% water by weight obtained with 2000 transients on a sample containing 46.4 mg.

population. This result demonstrates that the signal loss for the hydrated samples is associated with loss of cross-polarization efficiency.

To understand the basis for the signal loss further at hydration levels greater than 30% (w/w), the carbon signal intensity was measured as a function of contact time as shown in Figure 3. For the dry sample (B), the spectrum amplitude decreases at long contact times, but the spectra maintain their shape at different contact times, demonstrating that the spectrum is dynamically homogeneous. However, sample A at 39.8% water displays a broad spectrum at short contact times and decreased signal but narrow lines at long contact times. This change in spectral shape as a function of contact time is most readily interpreted in terms of local dynamic heterogeneity. The longer contact times select for the portions of the spectrum that have long relaxation times in the rotating frame and which are therefore more rigid. By comparison, the shorter contact time spectra are broader because more spins are represented, many of which relax more rapidly, thus giving a broader contribution to the spectrum. Thus, the short contact time spectrum or the 90° pulse spectrum is an accurate representation of all the spins in the sample, but both experiments suppress the fact that the sample is dynamically heterogeneous with some components far more mobile than others at the water content of 39.8%.

Though the signal-to-noise ratios appear similar in the A series of spectra, the number of transients required to obtain each spectrum is very different. This result is expected because the narrow components become visible when the broader components have decayed away and do not contribute to the signal. The heterogeneity, however, also implies that relaxation rates are not precisely defined. Thus, the spectral selection that leads to the narrow component spectrum in set A also requires a distribution of relaxation times, T_{IS} and T_{1rho}. It is very likely that both increases in T_{IS} and decreases in T_{1rho} are important in the loss of the cross-polarization signal. The lack of broad components in the A spectra at long contact times demonstrates the decline of T_{1rho}. The loss of the proton–carbon dipolar coupling is demonstrated at a somewhat higher water content by the fact that one may observe the carbon spectrum with the proton decoupler turned off as shown in Figure 5C.

The spectrum shown in Figure 1D is particularly interesting because it shows not only that sensitivity is lost in the cross-polarization experiment but also that the resolution is also

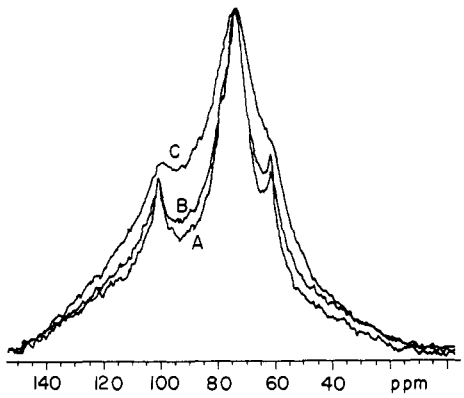

FIGURE 4: ^{13}C cross-polarization magic-angle-spinning spectra obtained at 50.3 MHz on a glycogen sample containing 39.8% water by weight as a function of the rotor frequency. 30-Hz line broadening was applied to each spectrum. (A) 25 900 transients at 3.5-kHz rotor frequency; (B) 26 500 transients at 1.0-kHz rotor frequency; (C) 24 800 transients obtained on a static sample.

Table II: Glycogen Carbon-13 Spin-Lattice Relaxation Times

hydration (wt %)	carbon-13 T_1 (s)				
	C_1	C_4	C_3	C_2, C_5	C_6
7.3	28.5	20.7		14.4	0.77
23.8	6.4	4.8		4.2	0.39
25.0 (D_2O)	7.9	5.7		4.5	0.3
72.7	0.14[a]	0.18[b]	0.19	0.18	0.086
shift (ppm)	100–103	82.5–77	73.8	72.5	61.0

[a] Chemical shift from 103 to 100 ppm observed at this hydration relative to 7.3% hydration. [b] Chemical shift from 82.5 to 77 ppm observed at this hydration relative to 7.3% hydration.

significantly degraded in the magic-angle spinning experiment at this water content. This observation is consistent with there being significant reorientation of the carbon atoms of the glucose ring on the time scale of the rotor period. That is, the system is not in either the fast mixing regime or the slow mixing regime with respect to the time scale of the rotor period, which was 0.4 ms in this case. This point is made more clear by the data in Figure 4 which show the MASS spectrum at three rotor speeds. The higher resolution at higher rotor speeds is due to the fact that the shorter rotor periods permit less time for motion to occur during the sample rotation. Any motion during the rotor period defeats the averaging of the first-order contributions to the broadening from the carbon chemical shift anisotropy or other dipolar contributions. Thus, motions on the time scale of the rotor period are apparent at 40% water content. At higher water content, however, spectral resolution is recovered, and by 60% water by weight, the spectrum approaches the solution limit. The spectra shown in Figure 5 obtained at 70% water demonstrate that the proton–carbon dipolar coupling is almost completely averaged, as the scalar coupling is apparent with the proton decoupler turned off. Similar scalar coupling may be observed in a static spectrum as well.

The carbon spin–lattice relaxation times, T_1, add further information about the hydration-induced dynamic response of the sample and are summarized in Table II. In the dry material, resolution of all carbon atoms is not achieved, but several classes of carbon atoms are still resolved. In the 7.3% water content sample, the carbon relaxation times are similar to those often observed for polymer systems; i.e., the relaxation times are in the tens of second range representing carbon atoms that are very largely immobilized and on the low-temperature side of the carbon T_1 minimum. In the present case, the C_6 carbon is unique in that the relaxation time is significantly shorter than the other carbons in the 7.3% hydrated material.

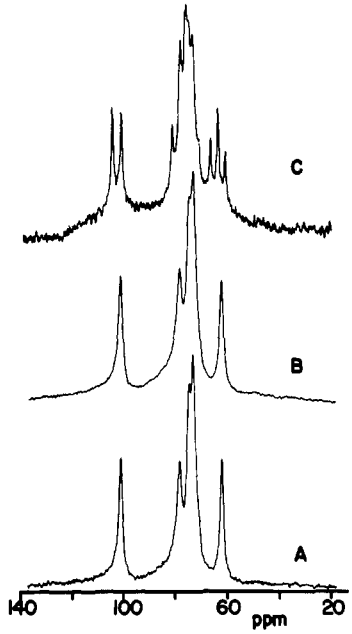

FIGURE 5: Static ^{13}C NMR spectra obtained at 50.3 MHz on hydrated glycogen samples under several acquisition conditions. (A) 71.8% water by weight obtained with 8100 90° pulses with dipolar ^1H decoupling and a 10-Hz line-broadening parameter. (B) 71.8% water by weight obtained with 22 560 90° pulses with scalar ^1H decoupling and a 10-Hz line-broadening parameter. (C) 72.7% water by weight obtained with 2689 90° pulses using no ^1H decoupling and a line broadening of 10 Hz.

This observation is consistent with rapid rotational motion of this group with respect to the ring. The fact that the C_1 and C_4 carbons have longer relaxation times than the other ring atoms may reflect some ring wobble about the 1–4 local axis which would also contribute to increased relaxation efficiency at C_6. It is interesting to note that the turning point for the most rapid dynamic changes appears to be associated with a mole ratio of water to glucose residues of 6, or one water molecule per oxygen atom.

Previous reports have indicated that in some polymer systems to which water has been added, the carbon T_1 change may be dominated by the effects of rapid local water molecule motion (Ganapathy et al., 1986). However, if this were the case in these samples, there would be a large difference in the efficiency of the carbon relaxation in H_2O compared with D_2O samples. The data in Table II show that this is not the case; only about 20% of the carbon relaxation can be associated with the intermolecular water proton–carbon interaction. Thus, the dominant feature of the water-induced change in the carbon T_1 is associated with changes in the local motions of the polymer itself.

In contrast to the dry samples, the carbon relaxation times for the 70% sample are all similar. The largest difference is approximately a factor of 2 between C_6 and the ring carbons; however, C_6 has two directly bonded protons while the others have only one, which, if other things are equal, would produce a factor of 2 difference in the relaxation rates. Thus, by 70% water, the motional averaging is so complete that all the carbon atoms in the polymer experience nearly the same correlation times. The values of the relaxation times measured for the 70% sample place the carbon spectrum close to the T_1 minimum at the resonance frequency of 50.3 MHz. Thus, the correlation times are in the range of a few nanoseconds.

Since the water contents of cells exceed the levels associated with this study, these data provide a useful background against which to examine in vivo carbon spectroscopy that may involve glycogen. The nonspinning spectra in Figure 5 demonstrate

clearly the basis for primary observability of the glycogen spectrum in vivo. That is, unlike macromolecules such as enzymes, the highly branched nature of the molecule provides a considerable amount of open space. This additional volume permits a very strong interaction with the solvent that leads to very efficient local motions which place the spectrum largely in the liquid limit. Motional averaging of the dipolar interactions is essentially complete. The difficult question remains that in vivo there may be some portion of the glycogen spectrum which is unobservable. Since there are many intermolecular interactions potentially present in the cell that could alter the molecular dynamics of the glycogen, it is not possible to address this question unequivocally by the present study. However, examination of the spectra in Figure 5 demonstrates that there is significant breadth in the carbon spectrum obtained under nonspinning conditions at the 70% water content that could make observation of part of the glycogen spectrum difficult. Hull and co-workers have reported this possibility on the basis of solution experiments as a function of temperature (Hull et al., 1987), and there is no basis in the present experiments to discount their conclusions that a relatively small fraction of the carbon C_1 resonances may be significantly broader than the others. It is likely that such a distribution of line widths would result from carbons in the regions of the branch points, where the motions are expected to be somewhat more constrained.

The response of glycogen is significantly different from other closely related polysaccharides such as starch which shows a heterogeneous response to hydration (Fyfe et al., 1984; Horii et al., 1986; Veregin et al., 1986). In the starch case, the crystalline regions become increasingly ordered with increasing hydration, while the noncrystalline regions lose signal intensity as observed in the glycogen experiments presented here. The origin of this difference is most likely associated with the highly branched glycogen structure that provides the solid with a considerable void volume which permits local motions more easily than the more densely packable structures. These data demonstrate that glycogen is a macromolecule that falls in the class of polymers which respond to water or solvent by dramatically increased local motion. This behavior is distinct from that observed using similar experiments conducted on enzymatic proteins where the response to the addition of water, as monitored by carbon and other rare spin NMR measurements, is very different (Marchetti et al., 1985; R. G. Bryant and S. D. Kennedy, unpublished). In the enzyme cases, the NMR spectrum may be maintained in very high resolution at high water contents. In fact, the resolution is higher in the highly hydrated state than in the dry lyophilized state. The proteins studied thus far, lysozyme and parvalbumin, fall in the class of molecules which respond to hydration by local reordering such that the local distribution of chemical shifts is very narrow in the hydrated state. The glycogen represents a class of molecules that have the opposite response; that is, the addition of water introduces considerable local motion that averages the local magnetic interactions in the solid and ultimately yields a solution-like sample.

Acknowledgments

We gratefully acknowledge useful discussions with Scott D. Kennedy.

Registry No. Glycogen, 9005-79-2.

References

Cael, J. J., Kwoh, D. L. W., Bhattacharjee, S. S., & Patt, S. L. (1985) *Macromolecules 18*, 819–821.

Canioni, P., Alger, J. R., & Shulman, R. G. (1983) *Biochemistry 22*, 4974–4980.

Cohen, S. M., Rognstad, R., Shulman, R. G., & Katz, J. (1981) *J. Biol. Chem. 256*, 3428–3432.

Demco, D. E., Tegenfeldt, J., & Waugh, J. S. (1975) *Phys. Rev. B 11*, 4133–4151.

Dubois, M., Gilles, K. A., Hamilton, J. K., Rebers, P. A., Smith, F. (1956) *Anal. Chem. 28*, 350–356.

Earl, W. L., & VanderHart, D. L. (1981) *Macromolecules 14*, 570–574.

English, A. D. (1985) *Macromolecules 18*, 178–181.

Fyfe, C. A., Stephenson, P. J., Taylor, M. G., Bluhm, T. L., Deslandes, Y., & Marchessault, R. H. (1984) *Macromolecules 17*, 501–502.

Ganapathy, S., Chacko, V. P., & Bryant, R. G. (1986) *Macromolecules 19*, 1021–1029.

Horii, F., Hirai, A., & Kitamaru, R. (1986) *Macromolecules 19*, 932–934.

Hull, W. E., Zerfowski, & Bannasch, P. (1987) Abstracts of the 6th Annual Meeting of the Society for Magnetic Resonance in Medicine, New York, p 488.

Marchetti, P. S., Ellis, P. D., & Bryant, R. G. (1985) *J. Am. Chem. Soc. 107*, 8191–8196.

Metzler, D. E. (1977) *Biochemistry, The Chemical Reactions of Living Cells*, Academic Press, New York.

Neurohr, K. J., Gollin, G., Neurohr, J. M., Rothman, D. L., & Shulman, R. G. (1984) *Biochemistry 23*, 5029–5035.

Pfeffer, P. E., Hicks, K. B., Frey, M. H., Opella, S. J., & Earl, W. L. (1984) *J. Carbohydr. Chem. 3*, 197–217.

Reo, N. V., Siegfried, B. A., & Ackerman, J. J. H. (1984) *J. Biol. Chem. 259*, 13664–13667.

Schaefer, J., & Stejskal, E. O. (1979) *Top. Carbon-13 NMR Spectrosc. 3*, 283–324.

Schaefer, J., Stejskal, E. O., Steger, T. R., Sefcik, M. D., & McKay, R. A. (1980) *Macromolecules 13*, 1121–1126.

Sillerud, L. O., & Shulman, R. G. (1983) *Biochemistry 22*, 1087–1094.

Stevens, A. N., Iles, R. A., Morris, P. G., & Griffiths, J. R. (1982) *FEBS Lett. 150*, 489–493.

VanderHart, D. L., & Atalla, R. H. (1984) *Macromolecules 17*, 1465–1472.

Veregin, R. P., Fyfe, C. A., Marchessault, R. H., & Taylor, M. G. (1986) *Macromolecules 19*, 1030–1034.